Elastic scattering of electrons by methane molecules

F. A. Gianturco,[1,*] J. A. Rodriguez-Ruiz,[2] and N. Sanna[3]
[1]*Department of Chemistry, The University of Rome, Città Universitaria, 00185 Rome, Italy*
[2]*Departamento de Quimica Fisica, Universidad de Malaga, Campus de Teatinos, 29071 Malaga, Spain*
[3]*Supercomputing Center for University Research, CASPUR, Città Universitaria, 00185 Rome, Italy*
(Received 14 November 1994)

Vibrational elastic, rotationally summed cross sections for electron collisions with CH_4 are calculated with *ab initio* static-exchange interactions and using a symmetry-adapted, single-center-expansion representation for the close-coupling equations. The correlation forces are included through density-functional theory and via a near-Hartree-Fock self-consistent-field description of the target wave function. Integral and differential cross sections are calculated over a broad range of collision energies, from the shape resonance region up to 50 eV. Comparisons with experiments and with previous calculations show that the present results indeed exhibit very good overall accord with measurements at these collision energies and describe very efficiently the electron angular distributions as given by a very broad range of measurements.

PACS number(s): 34.80.Bm

I. INTRODUCTION

Considerable progress has been made in recent years on both the theoretical and the experimental aspects of low-energy collisions of electrons with polyatomic molecules, after many years of rather slow progress with respect to that witnessed by the corresponding scattering processes from atomic targets. Such developments have been particularly remarkable for the CH_4 molecule, which has been studied by several groups over many years, becoming in a sense the testing system, similar to the hydrogen molecule in the case of diatomics, of both theories and experimental machineries for polyatomic targets. Methane is, of course, an important constituent of the atmospheres of the outer planets and is one of the key trace elements that could alter the upper atmosphere on earth, hence its relevance in molecular astrophysics [1]. Furthermore, it has become of interest for plasma processing [2], particularly for deposition processes, and also plays a relevant role in edge plasmas for fusion devices.

The observed cross sections in electron-methane scattering show a Ramsauer-Townsend minimum around 0.4 eV and a marked increase for higher energies with a maximum at about 8 eV. Both of those structures have been well examined by several experiments [3–14] in terms of integral cross sections, total, partial, and elastic, and in terms of differential cross sections at several collision energies and for a broad range of angles.

Calculations have also been carried out by several authors, who tested their theoretical models against the above experimental findings. Very extensive studies of electron-methane scattering were, in fact, published by Jain [15] using model potentials. Gianturco and Scialla [16] reproduced the Ramsauer-Townsend (RT) minimum in the integral cross section close to the experimental values, using a modified semiclassical exchange and a correlation-polarization potential from a free-electron-gas (FEG) model [17]. *Ab initio* results were obtained by the Schwinger multichannel method [18,19] and by using the complex Kohn variational (CKV) method [20]. The former calculations [18] provided differential cross sections at the static-exchange (SE) level and the static-exchange-plus-polarization (SEP) level of computation [19]. For the higher collision energies (between 7.5 and 20 eV) they found good agreement between calculated differential cross sections at the SE level and the experimental findings. At the SEP level, however, they found the RT minimum to be located at 0.1 eV. Similarly, the CKV calculations [20] obtained partial cross sections in the A_1, T_2, and E symmetry at the SE level and their resulting cross sections were in good agreement with the experimental results at higher energies. Further calculations with the same approach [21] at the SEP level, however, found the RT minimum at 0.4 eV, as the experiments suggest, and obtained computed differential cross sections for low collision energies (0.5–1.0 eV), which were also in good accord with the measurements.

Even more recently, model calculations on the CH_4 molecule have appeared [22] to describe the differential cross sections (DCS's) for the higher range of collision energies (10–50 eV) and found also reasonable accord with measurements. *Ab initio* calculations that employed an *ab initio* R-matrix (RM) treatment were also recently published [23] and reported the integral and partial elastic cross sections below the ionization limit and in the energy range of the experimental RT minimum. The corresponding DCS's were also computed in that region and found to be only in qualitative agreement with the measurements. It is interesting to note, however, that even the most sophisticated computational methods still show discrepancies with the experiments and indicate that a

*Author to whom correspondence should be addressed.

fully converged SEP calculation for the cross sections of this test molecule still needs to be done.

In the present paper we extent our earlier work on the methane molecule [6,7] by obtaining more accurately both the description of the target wave function and the exchange interaction between the scattering electron and the bound electrons. Furthermore, we test various types of correlation-polarization potential functions (V_{CP}) by employing different forms of density-functional theory (DFT) recently proposed by us for electron and positron scattering from atomic targets [24,25]. The aims of the calculations that we will report in this paper are therefore the following: (i) to employ the symmetry-adapted single-center expansion (SCE) of the total wave function within a close-coupling (CC) set of scattering equations starting with a multicenter wave function for the target electrons (this approach has been recently tested by us for other polyatomic molecules such as SiH_4 [26] and CF_4 [27] and found to yield very good agreement with experiments); (ii) to show that the inclusion of correlation effects via a DFT description of such forces is capable of giving final cross sections in quantitative accord with existing data and with a substantial reduction of computational effort with respect to more traditional multiconfigurational approaches; (iii) to test quantitatively the partial-wave expansion convergence of the SCE approach without the limitations of the single-center basis sets used before in the calculations [6,7]; (iv) to show that the use of an exact exchange treatment, i.e., the improved iterative exchange approach discussed earlier by us [27,28], allows us here to obtain integral and differential cross sections that show the best available agreement in the range of energy for the resonance feature and also at much higher scattering energies; and (v) to compare our computed DCS's, over a broad range of collision energies, with available experiments and with other recent computed values.

In the following section we describe our present computational approach, while Sec. III reports out integral cross sections for the rotationally summed, vibrationally elastic scattering processes and compares them with experiments and with other calculations. Section IV presents our calculated angular distributions and carries out the same sort of comparison, while our final conclusions are presented in Sec. V.

II. SINGLE-CENTER EXPANDED EQUATIONS

The initial step in our treatment is to generate the full electron-molecule interaction potential as a local and nonlocal function of the electronic density of the target molecule as given by its self-consistent-field (SCF) Hartree-Fock (HF) molecular orbitals (MO's) produced via a multicenter expansion over Gaussian-type analytic functions (GTO's) [29].

We describe the collisional process in terms of the solutions of the Schrödinger equation written in the form

$$\hat{H}\Psi(\mathbf{r},\mathbf{x})=E\Psi(\mathbf{r},\mathbf{x}) , \tag{1}$$

where

$$\hat{H}(\mathbf{r},\mathbf{x})=\hat{T}(\mathbf{r})+\hat{V}(\mathbf{r},\mathbf{x})+H_m(\mathbf{x}) , \tag{2}$$

with $\hat{T}$ being the kinetic energy operator for the scattering electron, $\hat{V}$ is the electron-molecule interaction, and $\hat{H}_m$ is the Hamiltonian of the molecular target. We let $\mathbf{x}$ represent collectively the coordinates of the bound electrons and of the molecular nuclei and intend to refer all particles to a frame of reference fixed to the molecule [body-fixed (BF) frame].

The many-body problem in the scattering, electronic coordinate $\mathbf{r}$ is now converted into an effective single-particle problem by expanding

$$\Psi(\mathbf{r},\mathbf{x})=\sum_{\alpha} A\{F_\alpha(\mathbf{r})\phi_\alpha(\mathbf{x})\} , \tag{3}$$

where A is the antisymmetrization operator for the electronic coordinates, while the molecular nuclei are considered as being fixed in space during the scattering event (FN approximation [30]).

By inserting Eq. (3) into Eq. (1) and multiplying the left-hand side by the conjugate of a representative state in the expansion (3), one obtains the familiar set of coupled integro-differential equations (IDE's)

$$\hat{H}_\alpha F_\alpha(\mathbf{r})=\sum_{\beta}\xi_{\alpha\beta}(\mathbf{r}) . \tag{4}$$

In the above set of (CC) equations for the scattering problem the following meaning of the symbols applies:

$$H_\alpha=\nabla_\alpha^2+k_\alpha^2 , \tag{5}$$

$$\xi_{\alpha\beta}(\mathbf{r})=\int \hat{K}_{\alpha\beta}(\mathbf{r}|\mathbf{r}')F_\beta(\mathbf{r}')d\mathbf{r}' , \tag{6}$$

$$K_{\alpha\beta}(\mathbf{r}|\mathbf{r}')=\hat{V}_{\alpha\beta}(\mathbf{r})\delta(\mathbf{r}-\mathbf{r}')+\hat{W}_{\alpha\beta}(\mathbf{r}|\mathbf{r}') . \tag{7}$$

Here k_α^2 is given by $2(E-\varepsilon_\alpha)$, with E being the total collision energy and ε_α the molecular internal energy in the target state $|\alpha\rangle$. The local interaction involves, in our treatment, the exact electrostatic interaction with the target $\hat{V}_{st}$ and the linear response function of its electrons to the impinging projectile, the correlation-polarization potential $\hat{V}_{CP}$, described in our earlier work [3] using the (FEG) approximation and recently further modified by using gradient expansion corrections to a (DFT) treatment of short-range correlation [24,25]. The nonlocal interaction $\hat{W}_{\alpha\beta}$ describes the exchange potential between the bound and the continuum orbitals, obtained exactly via energy-optimized iterative schemes [28]. In the case of only one single term in the expansion (3), the elastic scattering problem is then dealt with for a specific electronic state $|\alpha\rangle$ of the target molecule within the FN approximation [30].

In order to solve the numerical problem as that of a set of coupled integro-differential radial equations, one needs now to expand both the bound $[\Phi_i(\mathbf{x}_i)]$, multicenter MO's, and the continuum electron function $[F(\mathbf{r})]$ over a set of (SCE), symmetry adapted partial waves X:

$$\Phi_i(\mathbf{x}_i)=\sum_{h,l} r^{-1}u_{hl}^i(r)X_{hl}^{p_i\mu_i}(\vartheta,\varphi) , \tag{8a}$$

$$F_{p\mu}(\mathbf{r})=\sum_{h,l} r^{-1} f_{hl}^{p\mu}(r) X_{hl}^{p\mu}(\vartheta,\varphi) \ . \tag{8b}$$

Here $|i\rangle$ labels a specific, multicenter, occupied MO within the single-determinant description of the SCF HF wave function of the target molecule. The indices of the continuum function and of each contribution $|p\mu\rangle$ label a relevant irreducible representation (IR) p and one of its component μ. The index h labels a specific basis, for the given partial wave l, used within the pth IR one is considering. The generalized, symmetry-adapted harmonics was given before many times [5,6] and will not be discussed here again. The corresponding coefficients $u_{hl}^{i}=u_{hl}^{p_i\mu_i}(r)$ are the essential ingredients for computing the interaction potentials of Eq. (7) and were obtained here by numerical quadrature of the multicenter GTO's given as Cartesian Gaussian functions

$$g_{\nu}^{kj}(\mathbf{x}_k)=N(a,b,c;\alpha)x^a y^b z^c \exp(-\alpha x^2) \tag{9a}$$

labeled by the kth atomic center, of which g is the jth function, and by the contraction index ν of the primitive Gaussian within the subgroup that belongs to a given set of contraction coefficients d_ν

$$G^{kj}(\mathbf{x}_k)=\sum_{\nu=1}^{\nu_{\max}} d_{\nu}^{kj} g_{\nu}^{kj}(\mathbf{x}_k) \ . \tag{9b}$$

The remaining parameters are included in the normalization constant N:

$$N(a,b,c;\alpha) = \left[\frac{2}{\pi}\right]^{3/4} [(2a-1)!!(2b-1)!!(2c-1)!!]^{1/2} \times(\alpha)^{(a+b+c)/2+3/4} \ . \tag{10}$$

The corresponding radial coefficients of Eq. (8a) are thus given by the angular quadratures

$$u_{hl}^{i}(r;R)=\sum_{k\ \text{atoms}}\sum_{j\ \text{GTO's}}\sum_{v\ \text{coeffs}}\sum_{m}^{l}\int_0^{\pi}\sin\vartheta\, d\vartheta\int_0^{2\pi} b_{lm}^{i} S_{lm}^{i}(\vartheta,\varphi) C_{kj}^{i}(R) d_v^{kj} N(a,b,c;\alpha) x^a y^b z^c \exp(-\alpha x^2) d\varphi \ , \tag{11}$$

where the first two terms on the right-hand side describe explicitly the generalized real, symmetry-adapted harmonics X_{hl} with $|p\mu\rangle=|i\rangle$ and C_{kj} the GTO coefficient of the jth GTO. The quadratures where carried out via Gauss-Laguerre grids using a discrete, variable radial grid, for each point of which the spherical grid in the (ϑ,φ) points was evaluated. Convergence was achieved with grids of 46×46 sets of angular points, while up to 500 radial values were generated in the center of mass of the molecular target (BF frame). Several numerical tests were carried out using different grids and the final results can be considered converged (on the wave-function representation) within less than 1%. A further discussion of the accelerated convergence for the iterative exchange approach was already given in our previous work [26,2].

III. INTEGRAL ELASTIC CROSS SECTIONS

As mentioned in the Introduction, several experimental and theoretical data exist for the CH_4 molecule from electron scattering processes over a broad range of collision energies. It therefore becomes a very useful system for which to test the quality of the computational models one employs to describe the dynamics of the interaction.

The employed GTO, multicenter wave function was obtained using a quantum chemistry standard computer code [32] and was given by a triple-ζ expansion plus d-type polarization functions on C and p-type polarization functions on the H atoms. The bond distance was kept fixed at 2.063 a.u.

The SCE implementation was carried out, in a symmetry-adapted form, for all the potential contributions of Eq. (7) and for both the bound and the continuum orbitals of Eqs. (8), up to $l_{\max}=12$. The IR considered in the calculations were the A_1, the T_2, and the E symmetries for the continuum orbitals, while only the a_1 and the t_2 symmetries are occupied in the $^1A_1$ ground electronic state of the target molecule.

Convergence tests on the partial-wave expansions were carried out in all the symmetries. An example for the A_1 component is shown in Table I, where the computed integral elastic cross sections (rotationally summed) are shown for different $l_{\max}$ values. In that example the exchange interaction was given by a (FEG) local, energy-dependent approximation already discussed by us for polyatomic targets [29,31]. We have shown in Table I three l values only, i.e., the results for $l_{\max}=7$, 8, and 9: one clearly sees that all cross sections have essentially converged with $l_{\max}=7$, which means five coupled IDE's for the scattering process in the A_1 symmetry.

It is also interesting to note that, when using an approximate form for $\hat{W}_{\alpha\beta}$ in Eq. (7), it is usually suggested [33] that the continuum functions should be forced to be orthogonal to the bound orbitals of the same symmetry in order to guarantee the right nodal structure of all $N+1$ orbitals within the physical space of the molecular charge density. We have numerically tested the effects of such orthogonalization across the energy region of the broad shape resonance that exists in the CH_4 scattering process. Hence we have employed an energy-dependent local form of exchange model [34] with orthogonality constraints, while also carrying out calculations with exactly the same potential as before but without the enforcement of Lagrange multipliers: we found that the differences were rather small and only began to play a role when the energy went down to the (RT) minimum. This is rather reassuring since it means that approximate exchange interactions can still be used for semiquantitative treatments of the scattering problem.

The present results use the exact exchange interaction, whereby the final scattering orbitals at the (SE) level are

TABLE I. Computed partial integral sections (rotationally summed) for electron-CH_4 scattering in the $^2A_1$ state of the $(N+1)$-electron system. All quantities are in cm^2. The numbers in square brackets denote multiplicative powers of 10.

E_{coll} (eV) \ l_{max}	7	8	9
0.50	0.881 89[−16]	0.880 1[−16]	0.880 81[−16]
0.60	0.124 48[−15]	0.124 3[−15]	0.124 38[−15]
1.00	0.268 3[−15]	0.268 15[−15]	0.681 4[−15]
2.00	0.514 91[−15]	0.514 81[−15]	0.514 58[−15]
3.00	0.622 4[−15]	0.622 30[−15]	0.622 2[−15]
4.00	0.654 27[−15]	0.654 23[−15]	0.654 24[−15]
5.00	0.648 27[−15]	0.648 24[−15]	0.648 20[−15]
6.00	0.624 1[−15]	0.624 1[−15]	0.612 40[−15]
7.00	0.592 15[−15]	0.592 15[−15]	0.592 16[−15]
8.00	0.557 86[−15]	0.557 87[−15]	0.557 90[−15]
9.00	0.524 06[−15]	0.524 10[−15]	0.524 16[−15]
10.00	0.492 20[−15]	0.492 26[−15]	0.402 26[−15]
10.00	0.462 98[−15]	0.463 13[−15]	0.463 16[−15]
12.00	0.436 66[−15]	0.436 68[−15]	0.437 50[−15]
13.00	0.413 24[−15]	0.413 54[−15]	0.414 41[−15]
14.00	0.392 54[−15]	0.392 53[−15]	0.393 08[−15]
15.00	0.374 28[−15]	0.374 78[−15]	0.374 23[−15]

obtained correctly to be orthogonal to the bound MO's. They are shown in Fig. 1 for the present range of collision energies. The solid line shows the calculations using the GTO expansion discussed in the present work and the correlation-polarization potential from the DFT model [24]. The dashed line shows our calculations with a simpler correlation-polarization potential from the electron-gas model [17]. Finally, the dash-dotted curve reports calculations that used the FEG model and also employed directly our earlier single-center SCF wave function obtained from a Slater-type orbital basis set expansion [31,34]. One clearly sees that differences markedly exist around the resonance region and that the more flexible basis set exhibits very good agreement with the experiments that refer to elastic cross section measurements [20,21], the latter being the quantity produced by our calculations. The smaller basis set with the STO expansion, on the other hand, appears to provide the correct overall shape of the total integral cross sections as a function of energy, but it gives values about 10% larger in the 7–9 eV range of energies. It is worth noting at this point that the present results yield very accurate calculations for the CH_4 molecule, as we shall further discuss below. We have also shown in Fig. 1 the experimental points obtained for the total cross sections: filled squares are from Ref. [35] and open squares are from Ref. [36]. As expected, our better calculations using the present GTO expansion correctly produce elastic cross sections smaller than those given by the experiments that report the total cross sections. Further measurements for elastic cross sections are given by the filled triangles (Ref.[11]) and the open triangles (Ref. [9]). We see that our results that use the FEG modeling of correlation forces follow very closely such experimental data.

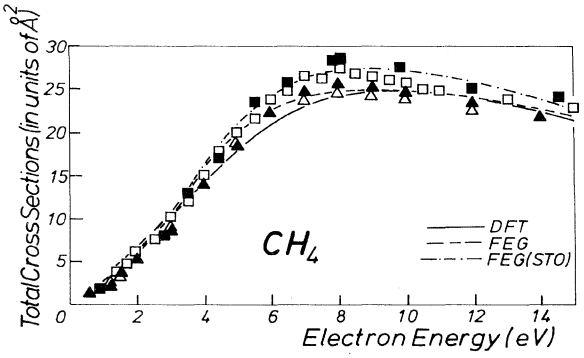

FIG. 1. Computed and measured elastic (rotationally summed) integral cross sections for electron-methane scattering. The experiments are represented as follows: filled squares, from Ref. [35]; open squares, from Ref. [36]; filled triangles, from Ref. [11]; open triangles, from Ref. [9]. The calculations are discussed in the main text.

It is interesting to see how the different *ab initio* models for the correlation-polarization potentials behave in the inner region, where different density-functional approaches could be used. The spherical components of the $V_{CP}(\mathbf{r})$ used in our present work are shown in Fig. 2. In the long-range region we employed the spherical component of the dipole polarizability coefficient, using its experimental value at the equilibrium geometry of the target [31]. The corresponding short-range potentials are given by the earlier FEG that uses the target density without gradient corrections [31,37] (dash-dotted line), by the density-functional theory with gradient corrections [24,25], and with two different choices of two-electron correlation function: the Lee-Yang-Parr model [38] and the Clementi-Carravetta model [39], both of which we have discussed at length before [40]. The latter model is given in Fig. 2 by a solid line, while the former is given by

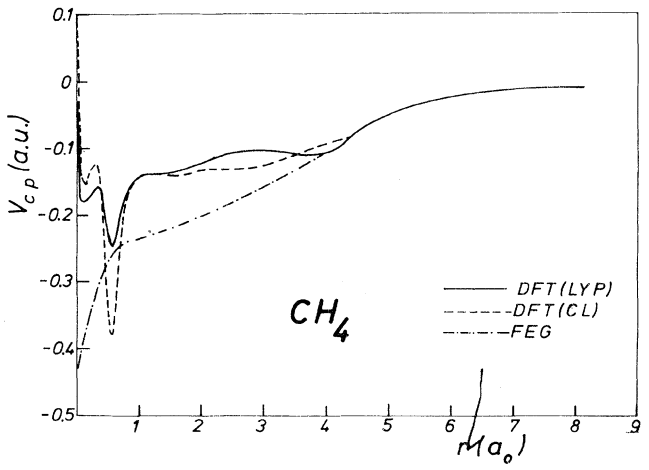

FIG. 2. Spherical components of the computed correlation-polarization potentials V_{CP} employed in the present calculations. The solid line refers to the DFT potential form of Ref. [36], the dashed curve gives the DFT with two different choices of the two-electron correlation function, and the dash-dotted curve gives the FEG model proposed in Ref. [37].

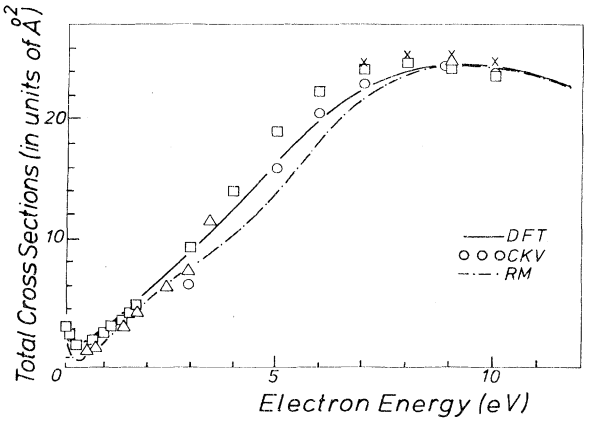

FIG. 3. Computed and measured integral elastic cross sections (rotationally summed) for electron scattering from CH_4. The experimental data are represented as follows: open squares, from Ref. [9]; crosses, from Ref. [11]; open triangles, from Ref. [12]. The calculations refer to the present results using DFT correlation potential, solid line; the RM calculations of Ref. [23], dash-dotted line; the CKV calculations of Ref. [21], open circles.

the dashed line. One clearly sees that the FEG modeling differs from the DFT approach in both the intermediate region of the interactions and in the very short distance behavior of the potentials, while the two different two-electron correlation functions appear to affect the V_{CP} mostly at very short distances.

As a result, the cross sections of Fig. 1 are essentially coincident for the case where DFT potentials are used (solid line), while the FEG results indicate differences in the intermediate-energy regions. One should keep in mind, on the other hand, that the short-range region of the V_{CP} potentials play a rather minor role because of the dominance there of nuclear Coulomb forces. The differences between the two models in the range of $2a_0-4a_0$, on the other hand, indicate that the FEG modeling of correlation forces produces a stronger contribution in that range of distances. All V_{CP} potentials, on the other hand, bring the computed cross sections rather close to the experimental findings. To further test the quality of the present calculations, the plots reported in Fig. 3 compare the experimental findings with our SCE results, which used exact static plus converged iterative exchange potentials (and further employed the present DFT model for correlation-polarization forces) with the most recent calculations that employed the (RM) approach [23]. Our data are given by the solid line for the DFT modeling of the V_{CP} potential. The RM results are given by the dash-dotted line. The experimental data are from the sets of references already shown in Fig. 1. One clearly sees that our DFT results follow very closely the elastic integral cross section data, while the RM results are consistently smaller in the low and intermediate ranges of energy and get closer both to experiments and to our calculations around the broad resonance maximum. It is also interesting to note that the rather extensive multiconfigurational calculations of Ref. [21], which used the CKV method mentioned before and are given by open circles in our figure, follow very closely the DFT results, but depart markedly from them as the energy gets lower. Given the rather limited computational effort needed to include the present V_{CP} model in our calculations, it is reassuring to see how well it performs in comparison both with experiments and with other much more complicated calculations.

If one further considers the fact that the experiments involved total integral cross sections and that the inelastic contributions around the RT region are estimated to be of the order of 50% of the total cross section [41], then one finds that our elastic cross-section values (rotationally summed but vibrationally elastic) are remarkably close to experiments as the collision energy decreases. Furthermore, we also see that the choice of our two models for the V_{CP} interaction affects rather little the overall energy dependence of the cross sections in Fig. 3 and makes also rather little difference in their magnitude. Both the DFT and the FEG calculations show a marked minimum at lower energy and agree very well with the experimental data, as we discuss elsewhere [42]. An extensive comparison between the present SCE approach and all the available recent calculations on the total integral elastic (rotationally summed) cross sections around the RT minimum shows, in fact, that the present approach indeed agrees well with both experiments and the best existing calculations. In conclusion, the calculations reported in this section, and the comparisons carried out with the existing experiments and with the most recent calculations using different methods, indicate that the present modeling of correlation forces by basically using a local density-functional approach, when coupled to the correct treatment of static and exchange forces, can yield rather good accord with experiments and appears to be very competi-

tive with respect to other, more complicated, modelings that use L^2-function expansions.

IV. SCATTERING ANGULAR DISTRIBUTIONS

As mentioned earlier, the behavior of the angular distributions of various collision energies, when compared with experimental data, becomes a very useful indicator of the quality of a given computational model. As we shall see in this section, this is particularly true for the measurements available for the methane molecule.

We present in Fig. 4 the behavior of the elastic cross sections at 10 eV, together with the results of the measurements and of earlier calculations. The experimental data are from Boesten and Tanaka [13] (filled circles) and from Shyn and Cravens [14] (open circles). The calculated values are the present results using the DFT model (solid line), the FEG model (dashed line) to treat correlation effects, and the earlier SCE calculations from Thompson, McNaughten, and Jain [43] (short-dashed line). As one can see, both our calculations produce essentially the same results at such energies and follow very closely the experiments of Boesten and Tanaka: the earlier results [43] are larger than the measured data at all angles but follow as well as our calculations their general shape. It is interesting to note that the recent SCE calculations with model potentials [22] are also as close to experiments as our results and indicate a remarkable agreement among different theoretical approaches as far as the present DCS is concerned.

Two higher collision energies are examined by the calculations and measurements reported in Figs. 5 and 6. In the data of Fig. 5 the results shown refer to an E_{coll} value of 15 eV, while those from Fig. 6 show elastic DCS's at 20 eV. The experimental data are, in both cases, from the references mentioned before [13,14]. Our calculated

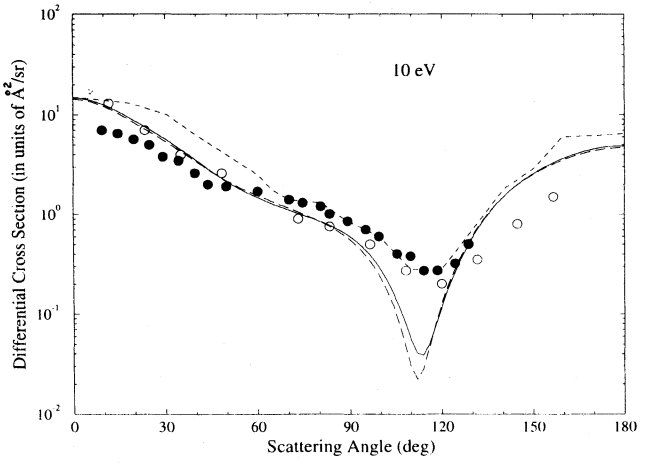

FIG. 4. Computed and measured differential cross sections at 10 eV. Only rotationally elastic cross sections are shown. The experimental data are represented as follows: filled circles, from Ref. [13]; open circles, from Ref. [14]. The present calculations are represented as follows: solid line, using the DFT model; long-dashed line, using the FEG model. The calculations of Ref. [43] are given by the short-dashed line.

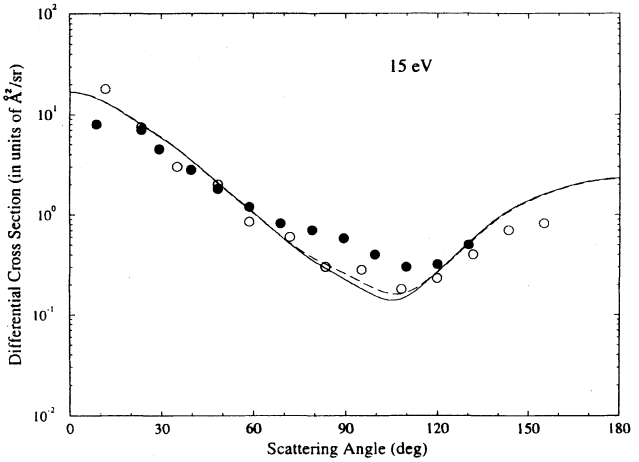

FIG. 5. Same as in Fig. 4 but for a collision energy of 15 eV. The meaning of the symbols is the same as in Fig. 4.

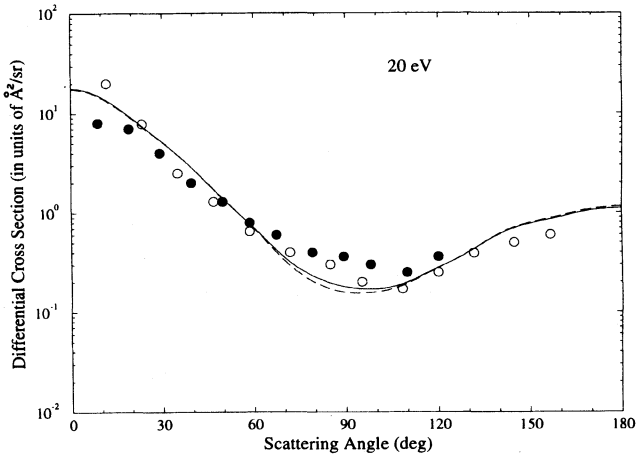

FIG. 6. Same as in Fig. 4 but for a collision energy of 20 eV.

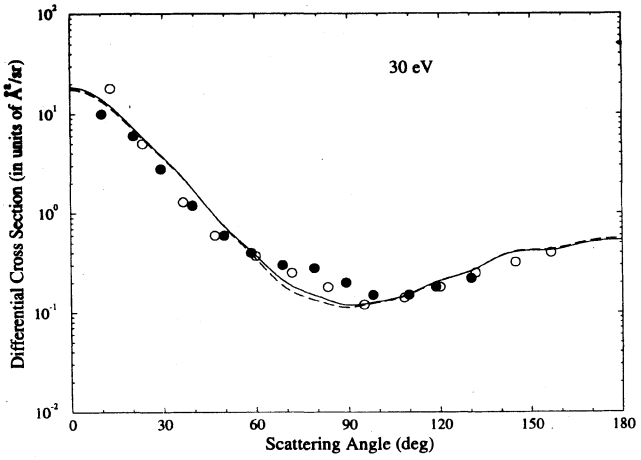

FIG. 7. Same as in Fig. 4 but for a collision energy of 30 eV.

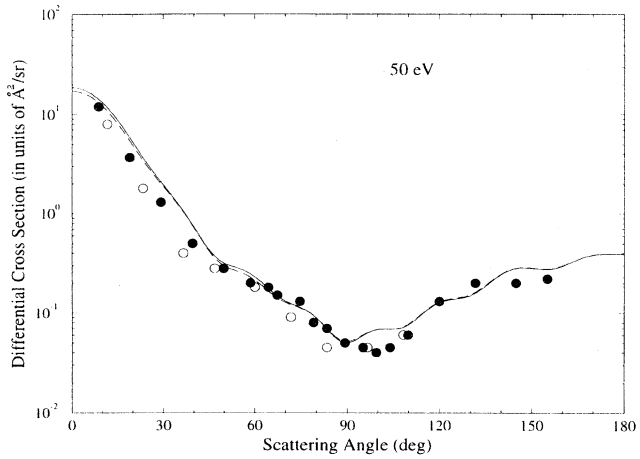

FIG. 8. Same as in Fig. 4 but for a collision energy of 50 eV.

quantities follow again very closely the measured data and show at both energies minima in the DCS that coincide with the experiments. The recent model calculations of Nishimura and Itikawa [22] are also very close to measurements as far as overall shape of the DCS is concerned, but are consistently slightly smaller than our cross sections.

A further set of calculations and measurements, at two higher collision energies, is reported in Figs. 7 and 8, where the former refers to an E_{coll} value of 30 eV while the latter is for a value of 50 eV. The experiments are again from the previous references [13,14]. Our two different models of the correlation forces once more give results that are practically coincident at all angles. This is in keeping with calculations at low energies [42], where it was shown that the two models affect the results only at very low collision energies and there only over a limited range of angles. Furthermore, it stands to reason that, as the collision energy increases, the electron penetrates more deeply inside the molecular charge distribution and therefore the V_{st} and the W_{exch} contributions dominate the scattering process. It is also very reassuring to see that our calculations provide very good accord with experiments at all the scattering angles, i.e., up to very large ϑ values as given by the experiments. The earlier, more elaborate calculations of elastic DCS [21,43] showed in one case [21] results up to only 7.5 eV, while the others [43] are usually too large in the smaller-angle region of the DCS. The more recent SCE model calculations at the same collision energies [22] also show much larger contributions as the scattering angles increase and therefore indicate stronger backscattering effects with respect to experiments. Both calculations [22,43] therefore produce momentum transfer cross sections Q_m that are markedly larger than the experiments [22]. Our present results, on the other hand, show better accord with existing data and produce much smaller Q_m values at the collision energies of the measurements [13,14]. A comparison for such

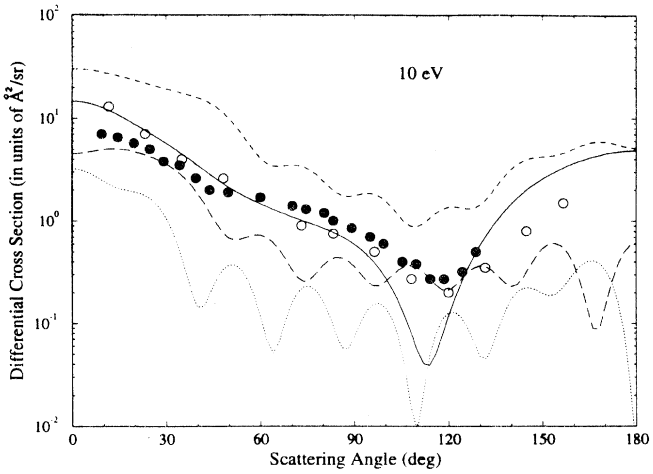

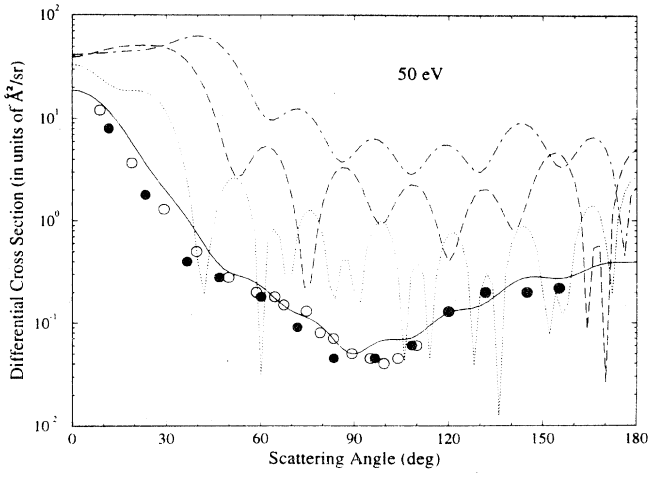

FIG. 9. Computed state-to-state rotationally inelastic cross sections at 10 eV (top) and at 50 eV (bottom) of collision energy. Solid line, 0→0 process; long-dashed line, 0→4 excitation; dotted line 0→3 excitation; dashed line, total, rotationally summed cross section. The experimental data are represented as in Fig. 4.

TABLE II. Computed and measured momentum transfer cross sections Q_m in units of Å^2 (elastic values).

Energy (eV)	5.0	10.0	15.0	20.0	30.0	50.0
Present (FEG) 14.4	14.4	15.1	9.53	6.54	4.00	2.39
Present (DFT)	13.5	14.8	9.53	6.51	3.95	2.38
From Ref. [22]		15.83	11.97	9.05	6.02	3.42
Expt. from Ref. [14]		10.05	7.5	5.4	3.5	1.8
Expt. from Ref. [13]		20.21	11.78	6.95	3.87	2.22

quantities is shown in Table II.

It is also interesting to discuss at this point the possible role of inelastic processes at the collision energies examined in this work. As an example for such an analysis we report in Fig. 9 two sets of state-to-state rotationally inelastic cross sections at 10 eV (top part of the figure) and at 50 eV (bottom part of the figure). One clearly sees that, depending on the angle, some of the processes show inelastic contributions larger than the elastic one. In particular, at 10 eV one sees that the $0 \rightarrow 4$ excitation contributes substantially around the minimum shown both by experiments and, more markedly, by our $0 \rightarrow 0$ calculations. Given the fact that the experiments measure the elastic process, as their close agreement with our calculations clearly show, one cannot rule out the possibility that some inelastic effects are also present in the experiments around 110°, thus explaining the differences with our calculations at those angles. An even clearer example of the increased role of inelastic processes as the energy increases is shown by the results at 50 eV, reported in the bottom part of Fig. 9. One clearly sees now that the experiments definitely refer to the elastic process since inelasticity now plays a much larger role and would dominate the scattering process.

V. CONCLUSIONS

In the present work we have analyzed in some detail the behavior of integral and differential elastic cross sections for electron scattering from CH_4 at collision energies from the broad T_2 resonance around 8 eV up to 50 eV. The computational procedure that we employ here starts from a multicenter description of the target molecule and proceeds to solve the scattering problem using a single-center close-coupling expansion in symmetry-adapted angular functions. The method turns out to be computationally feasible not only for such a special target molecule, but also for a more complex case such as CF_4 [44], SF_6 [45], and benzene [45]. The treatment of the interaction is carried out at the *ab initio* level for the V_{st} and the W_{exch} so that essentially exact SE cross sections can be obtained. Correlation and polarization forces, on the other hand, are treated via a parameter-free *ab initio* model that uses a local density-functional modeling of short-range dynamic correlation. The present calculations, like earlier ones [17,26,27], indicate that such models work well for the electronic ground-state and for systems where the static correlation effects are rather unimportant. They correctly describe the final cross-section behavior down to very low collision energies [42] and over a broad range of angles and energies, as shown in this work. Given the reduction in computational effort, such an approach seems indeed to be very promising for treating larger molecular targets and for the formulation of realistic local models of electron-molecule interactions in the study of shape resonance effects. A detailed analysis for the SF_6 molecule, in fact, has been recently completed in our laboratory [45].

In the present calculations we have also shown that our computational model can provide quantitative agreement with existing data as well as any of the more complicated computational methods and often better than them for crucial features in the cross sections [42], both integral and differential. Extensions to the treatment of vibrational inelastic processes are currently under study and will be presented elsewhere [46].

ACKNOWLEDGMENTS

The financial support of the Italian National Research Council, the Italian Ministry for University and Research, and the European Union through its Human Capital and Mobility (HCM) program is gratefully acknowledged. One of us (J.A.R.R.) also thanks the HCM program for financial support.

[1] See, e.g., S. K. Atreya, *Atmospheres and Ionospheres of the Outer Planets and their Satellites* (Springer-Verlag, Berlin, 1986).
[2] W. L. Morgan, Plasma Chem. Plasma Process. **12**, 477 (1992).
[3] R. B. Brade, Phys. Rev. **25**, 636 (1925).
[4] E. Brüche, Ann. Phys. (Leipzig) **83**, 1065 (1927).
[5] E. Brüche, Ann. Phys. (Leipzig) **4**, 387 (1930).
[6] C. Ramsauer and R. Collath, Ann. Phys. (Leipzig) **4**, 91 (1930).
[7] E. Barbarito, M. Basta, and M. Calicchio, J. Chem. Phys. **71**, 54 (1979).
[8] H. Tanaka, T. Okada, L. Boesten, T. Suzuki, T. Yamamoto, and M. Kubo, J. Phys. B **15**, 3305 (1982).
[9] J. Ferch, B. Granitza, and A. Raith, J. Phys. B **18**, L445 (1985).
[10] R. K. Jones, J. Chem. Phys. **82**, 5424 (1985).
[11] B. Lohmann and S. J. Buckmann, J. Phys. B **19**, 2565 (1986).
[12] W. Sohn, K. H. Kochem, K.-M. Scheuerlein, and H. Ehrhardt, J. Phys. B **19**, 3625 (1986).
[13] L. Boesten and H. Tanaka, J. Phys. B **24**, 821 (1991).
[14] T. W. Shyn and T. E. Cravens, J. Phys. B **23**, 293 (1990).
[15] A. Jain, Phys. Rev. A **34**, 954 (1986).
[16] F. A. Gianturco and S. Scialla, J. Phys. B **20**, 3171 (1987).
[17] F. A. Gianturco, A. Jain, and L. C. Pantano, J. Phys. B **20**, 571 (1987).
[18] M. A. P. Lima, T. L. Gibson, W. M. Huo, and V. McKoy, J. Phys. A **32**, 2696 (1985).
[19] M. A. P. Lima, K. Watari, and V. McKoy, Phys. Rev. A **39**, 4312 (1989).
[20] C. W. McCurdy and T. N. Rescigno, Phys. Rev. A **39**, 4487 (1989).
[21] B. M. Lengsfield III, T. N. Rescigno, and C. W. McCurdy, Phys. Rev. A **44**, 4296 (1991).
[22] T. Nishimura and Y. Itikawa, J. Phys. B **2**, 2309 (1994).

[23] B. M. Nestmann, K. Pfingst, and S. D. Peyermhoff, J. Phys. B **27**, 2297 (1994).
[24] F. A. Gianturco and J. A. Rodriguez-Ruiz, Phys. Rev. A **47**, 1075 (1993).
[25] F. A. Gianturco, A. Jain, and J. A. Rodriguez-Ruiz, Phys. Rev. A **48**, 4321 (1993).
[26] F. A. Gianturco, R. B. Lucchese, N. Sanna, and A. Talamo, in *Electron Scattering from Molecules, Surfaces and Clusters,* edited by H. Ehrhardt and L. Morgan (Plenum, New York, 1994).
[27] F. A. Gianturco, R. B. Lucchese, and N. Sanna, J. Chem. Phys. **100**, 6464 (1994).
[28] A. Jain, F. A. Gianturco, and D. G. Thompson, J. Phys. B **24**, L255 (1991).
[29] F. A. Gianturco, V. Di Martino, and A. Jain, Nuovo Cimento D **14**, 411 (1992).
[30] A. Temkin and K. V. Vasavada, Phys. Rev. **160**, 109 (1967).
[31] F. A. Gianturco, A. Jain, and L. C. Pantano, J. Phys. B **20**, 71 (1987).
[32] HONDO Version 7.0, Dupuis-Watts-Villar-Hurst, 1987.
[33] T. L. Gibson and M. A. Morrison, J. Phys. B **14**, 127 (1981).
[34] F. A. Gianturco and S. Scialla, J. Phys. B **20**, 3171 (1987).
[35] M. S. Dababneh, Phys. Rev. A **38**, 1207 (1988).
[36] A. Zecca, G. Karwasz, R. S. Brusa, and C. Szmytkowski, J. Phys. B **24**, 2747 (1991).
[37] N. T. Padial and D. W. Norcross, Phys. Rev. A **29**, 1742 (1984).
[38] C. Lee, W. Yang, and R. G. Parr, Phys. Rev. B **37**, 785 (1988).
[39] E. Clementi and V. Carravetta, J. Chem. Phys. **81**, 2646 (1984).
[40] F. A. Gianturco and J. A. Rodriguez-Ruiz, J. Mol. Struct. (Theochem) **260**, 99 (1992).
[41] D. Field (private communication).
[42] F. A. Gianturco, J. A. Rodriguez-Ruiz, and N. Sanna, J. Phys. B **28**, 1287 (1995).
[43] P. Mc Naughten, D. G. Thompson, and A. Jain, J. Phys. B **23**, 2405 (1990).
[44] F. A. Gianturco, R. B. Lucchese, and N. Sanna, J. Chem. Phys. **102**, 5743 (1995).
[45] F. A. Gianturco and R. B. Lucchese, Int. Rev. Phys. Chem. (to be published).
[46] S. Althorpe and F. A. Gianturco, J. Phys. B (to be published).